Structural Determinants of Ion Flow Through Recombinant Glutamate Receptor Channels

TODD A. VERDOORN,* NAIL BURNASHEV, HANNAH MONYER, PETER H. SEEBURG, BERT SAKMANN†

Functional glutamate receptors (GluRs) were transiently expressed in cultured mammalian cells from cloned complementary DNAs encoding GluR-A, -B, -C, or -D polypeptides. The steady-state current-voltage (*I-V*) relations of glutamate- and kainate-induced currents through homomeric channels fell into two classes: channels composed of either the GluR-A, -C, and -D subunits showed doubly rectifying *I-V* curves, and channels composed of the GluR-B subunits displayed simple outward rectification. The presence of GluR-B subunits in heteromeric GluRs determined the *I-V* behavior of the resulting channels. Site-directed mutagenesis identified a single amino acid difference (glutamine to arginine) in the putative transmembrane segment TM2 responsible for subunit-specific *I-V* relationships. The properties of heteromeric wild-type and mutant GluRs revealed that the dominance of GluR-B is due to the arginine residue in the TM2 region.

THE α-AMINO-3-HYDROXY-5-METHYL-4-isoxazolepropionic acid (AMPA) receptor subtype of neuronal glutamate receptors (*1*) is thought to mediate a large proportion of fast excitatory synaptic transmission in the central nervous system. Several cDNAs encoding a family of homologous GluR subunits of the AMPA type have been isolated. These polypeptides form homo- and heteromeric recombinant GluR channels having subunit- and splice-specific properties when expressed in host cells (*2–7*). The extent of functional GluR-channel diversity in native membranes, the subunit stoichiometry of GluR channel subtypes, and the functionally important domains of the subunits are unknown. Using site-directed mutagenesis and functional analysis of recombinant GluR channels, we have identified subunits and subunit domains important for the conductance properties of GluR channels.

Subunit-specific differences between GluR channels were revealed when *I-V* relations of homomeric channels were measured in human embryonic kidney cells expressing each of the four GluR polypeptides (*8*). Rapid application of 300 μM L-glutamate to cells expressing homomeric GluR-A, -B, -C, and -D receptors of the flip version (*7*) produced a peak current that rapidly decayed to a steady-state value. The peak current amplitude ranged from 2.5 to 8 times as large as that of the steady state current. The *I-V* relations for homomeric GluR-A channels showed a marked inward rectification starting near a membrane potential of 0 mV, similar to the *I-V* relations for GluRs expressed in *Xenopus* oocytes (*4, 5*). Outward rectification was observed at potentials more positive than +60 mV, giving rise to a doubly rectifying *I-V* curve (Fig. 1A). In contrast, currents mediated by homomeric GluR-B channels showed simple outward rectification (Fig. 1B). For each type of homomeric channel, the *I-V* curve of the peak current had the same shape (*9*) as that of the steady-state current. Steady-state *I-V* curves constructed by the voltage ramp method (*10*) indicated that homomeric GluR-A, -C, or -D channels all exhibited similar complex inward and outward rectification, whereas GluR-B channels gave simple outward rectification (Table 1).

Coexpression of GluR-A and -D subunits resulted in the formation of heteromeric channels (referred to as GluR-A/D channels) that displayed doubly rectifying *I-V* curves as expected from the *I-V* relations characterizing the homomeric channels of the constituting subunits (Fig. 1C). In contrast, channels formed by the combination of GluR-A and -B subunits (GluR-A/B) behaved similarly to homomeric GluR-B channels (Fig. 1D) (*4, 5*). Voltage ramp experiments revealed that coexpression of dual combinations produced channels showing simple outward rectification only if GluR-B was part of the receptor (Table 1). Otherwise, doubly rectifying *I-V* relations were observed. This suggests that the GluR-B subunit, when assembled with other subunits into heteromeric channels, determines the *I-V* behavior of the assembly.

The similar shapes of the GluR-B and GluR-A/B *I-V* relations indicate that few, if any, homomeric GluR-A channels are formed on coexpression of GluR-A and GluR-B. Other aspects of desensitization and its voltage dependence indicate that GluR-A/B are unique entities with properties different from those of homomeric channels formed from GluR-A or GluR-B. The peak and steady-state I-V curves were different in GluR-A/B combinations (Fig. 1D), unlike in homomeric GluR-A (Fig. 1A) and -B (Fig. 1B) channels or the GluR-A/D combination (Fig. 1C). We tested the ratio of chord conductances at +80 and −80 mV (G_{+80}/G_{-80}), which is a measure of the voltage dependence of agonist-activated currents. In five cells expressing GluR-A/B channels to which 300 μM L-glutamate was rapidly applied, this ratio was 1.77 ± 0.26 (SEM) for the peak current and 2.72 ± 0.40 for the steady-state component ($P < 0.05$, paired *t*-test), suggesting that the initial,

Table 1. *I-V* relations of wild-type GluRs. Summary of data obtained from steady-state *I-V* curves determined by the voltage ramp method for various recombinant GluR channels composed of wild type subunits. The values represent the mean ± SEM determined for the number of cells indicated in parentheses. Reversal potentials (V_{rev}) were determined for L-glutamate–activated currents. V_{rev}, G_{+80}, and G_{-80} were determined as described (*9*). The ratio G_{+80}/G_{-80} reflects the shape of the *I-V* relations. Ratios less than 1 indicate inward rectification between −80 mV and +80 mV, whereas ratios greater than 1 are the result of outward rectification. The complex inward and outward rectifying *I-V* curves give ratios that are significantly less than 1. ND, not determined.

Subunit	V_{rev} (mV)	G_{+80}/G_{-80}	
		L-Glutamate (300 μM)	Kainate (300 μM)
GluR-A	−9.0 ± 3.6 (5)	0.070 ± 0.045 (5)	0.206 ± 0.125 (7)
GluR-B	−3.2 ± 2.5 (5)	2.65 ± 0.51 (5)	2.87 ± 1.04 (4)
GluR-C	−8.6 ± 4.3 (4)	0.219 ± 0.138 (4)	ND
GluR-D	−5.5 ± 3.9 (5)	0.125 ± 0.034 (5)	0.122 ± 0.048 (5)
GluR-A/B	−3.3 ± 2.7 (5)	2.02 ± 0.27 (5)	1.90 ± 0.14 (9)
GluR-A/C	−14 (1)	0.45 (1)	ND
GluR-A/D	−8.7 ± 3.9 (5)	0.108 ± 0.037 (4)	0.090, 0.100 (2)
GluR-B/C	4.7 ± 2.9 (4)	1.50 ± 0.46 (4)	ND
GluR-B/D	−2.4 ± 2.0 (9)	2.20 ± 0.16 (9)	2.28 ± 0.46 (4)

T. A. Verdoorn, N. Burnashev, B. Sakmann, Max-Planck-Institut für medizinische Forschung, Abteilung Zellphysiologie, Jahnstrasse 29, W-6900 Heidelberg 1, Federal Republic of Germany.
H. Monyer and P. H. Seeburg, Center for Molecular Biology at the University of Heidelberg (ZMBH), Laboratory for Molecular Neuroendocrinology, Im Neuenheimer Feld 282, W-6900 Heidelberg 1, Federal Republic of Germany.

*Present address: Department of Pharmacology, Vanderbilt University, Nashville, TN 37232.
†To whom correspondence should be addressed.

rapidly desensitizing peak current in heteromeric GluR-A/B channels is mediated by a different channel conformation than the steady-state current (*11*). The rate of desensitization induced by 300 μM L-glutamate at −60 mV was also significantly different between homomeric GluR-A and GluR-B and heteromeric GluR-A/B. In each case, desensitization proceeded by a single exponential decay, with GluR-A channels showing the fastest desensitization (decay time constant τ = 6.50 ± 0.56 ms, n = 9), GluR-B showing the slowest (τ = 35.9 ± 9.8 ms, n = 3), and GluR-A/B showing an intermediate desensitization time course (τ = 16.9 ± 2.3 ms, n = 6) (Fig. 1). Thus, the currents observed in cells expressing GluR-A/B were not simply the sum of currents mediated by homomeric GluR-A and GluR-B channels.

Homomeric GluR-B channels appear to mediate ion flow differently than do channels formed by GluR-A, -C, or -D subunits, and the presence of the GluR-B subunit seems to determine the *I-V* relation of heteromeric channels. The putative transmembrane region TM2 is identical in each of the four GluR polypeptides, except that GluR-B carries a positively charged arginine residue (R) at amino acid position 586 [GluR-B (R586)], whereas a glutamine residue (Q) with a neutral charge is found in the homologous position in GluR-A (Q582), -C (Q590), and -D (Q587) (Fig. 2A). We used site-directed mutagenesis (*12*) to replace the arginine in the GluR-B subunit with a glutamine, creating the mutant subunit GluR-B(R586Q). The GluR-D subunit was also mutated by changing the glutamine at position 587 to an arginine, yielding the mutant subunit GluR-D(Q587R). The shapes of the *I-V* curves produced on expression of mutant homomeric GluR-B or -D subunits were completely reversed (Fig. 2, B and C). The mutant GluR-B(R586Q) channel showed complex rectification, whereas the mutant GluR-D(Q587R) channels had an outwardly rectifying *I-V* relation, which is the opposite of the behavior seen with the wild-type subunits.

Because the steady-state *I-V* relation of heteromeric GluR channels is similar to that of homomeric GluR-B channels, we wished to determine if this "dominance" is conferred by the GluR-B subunit (that is, because multimeric receptors assemble with an excess of GluR-B subunits) or if the presence of an arginine in TM2 dominates the properties of the heteromeric assembly. We thus examined the *I-V* relation of heteromeric combinations in which one or both of the constituting subunits carried a mutation in TM2 (Fig. 3 and Table 2). The results indicate that heteromeric assemblies exhibit outwardly rectifying *I-V* relations if a subunit carrying the arginine is present, regardless of whether that subunit is the wild-type GluR-B or the mutant GluR-D. This is shown most clearly in channels formed by combination of both mutants. Thus, heteromeric GluR-B(R586Q)/D(Q587R) channels gave clear outward rectification (Fig. 3B) that was nearly indistinguishable from that of the corresponding wild-type combination (Fig. 3A). However, combinations lacking an arginine in the TM2 segment [for example, GluR-B(R586Q)/D (Fig. 3A)] always showed complex rectification behavior (Table 2).

The shape of whole-cell *I-V* relations is determined by the voltage dependence of the single channel conductance and by the voltage dependence of the open-close equilibrium. To determine the basis of the subunit-specific *I-V* relations, we used voltage jump experiments (*13*). Voltage dependence

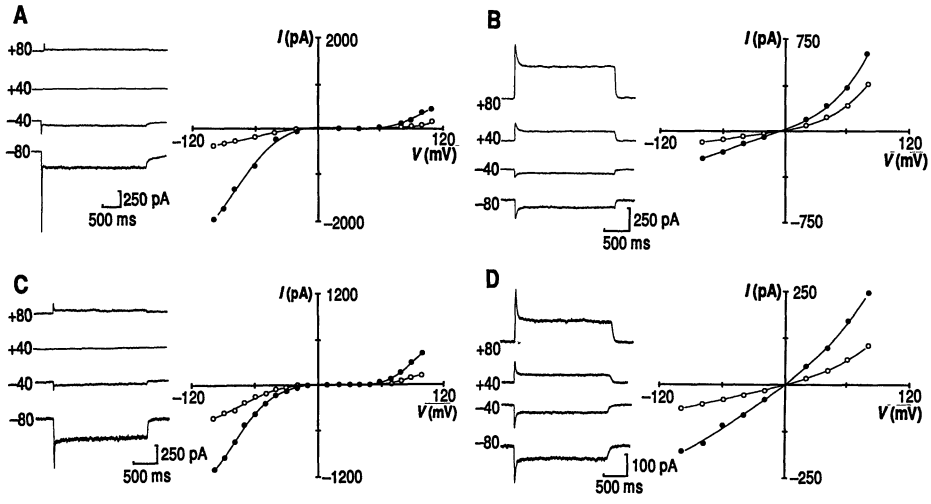

Fig. 1. Subunit dependence of the *I-V* relation mediated by recombinant GluR channels. Experiments were performed on cells expressing single subunits GluR-A (**A**) and GluR-B (**B**) or combinations of subunits GluR-A/D (**C**) and GluR-A/B (**D**). *I-V* curves were constructed by rapid application of 300 μM L-glutamate at various holding potentials. In each section current records are shown on the left, and the resulting *I-V* curves for the peak current (●) and the steady-state current (○) are shown on the right. The lines are the result of fitting the data points to polynomials (*9*). These results are representative of similar experiments performed on three to four cells in each case.

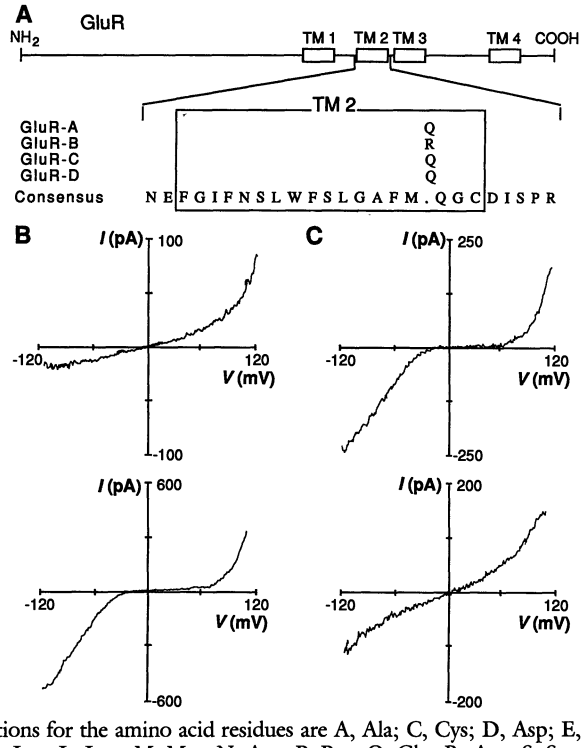

Fig. 2. Effect of a single amino acid difference in the transmembrane segment TM2 on the shape of the steady-state *I-V* relation. (**A**) A schematic diagram of the primary structure of a single GluR subunit indicating the location of the four putative transmembrane regions is shown at the top. Below is an expanded portion of the amino acid sequence surrounding TM2. Only one amino acid residue differs in this region (in GluR-B the R is at position 586, and in GluR-D the Q is at position 587). For complete sequences see (*2*). (**B**) The effects on *I-V* relations of mutation of wild-type GluR-B (top) to GluR-B(R586Q) (bottom). Each *I-V* curve was produced by the voltage ramp method (*8*) on a single cell. (**C**) Experiment similar to that performed in (B), with wild-type GluR-D (top) and mutant GluR-D(Q587R) (bottom). L-Glutamate (300 μM) was used to activate currents in each experiment. These and similar *I-V* curves were used to calculate the ratio of chord conductances, which are summarized in Tables 1 and 2. Single-letter abbreviations for the amino acid residues are A, Ala; C, Cys; D, Asp; E, Glu; F, Phe; G, Gly; H, His; I, Ile; K, Lys; L, Leu; M, Met; N, Asn; P, Pro; Q, Gln; R, Arg; S, Ser; T, Thr; V, Val; W, Trp; and Y, Tyr.

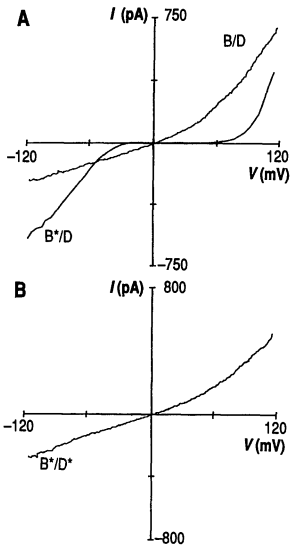

Fig. 3. The arginine residue in the transmembrane segment TM2 dominates the behavior of heteromeric channels. (**A**) Superimposed steady-state *I-V* curves constructed by the ramp method in two cells expressing either heteromeric GluR-B/D or GluR-B(R586Q)/D (GluR-B*/D) channels. (**B**) *I-V* curve measured from a cell expressing a heteromeric combination of mutant GluR-B(R586Q) and GluR-D(Q587R) (GluR-B*/D*). This heteromeric combination also contains an arginine, contributed by GluR-D(Q587R).

of the channel conductance should be observed in the instantaneous *I-V* relation when the current amplitudes are measured immediately after the voltage jump, whereas the relaxation of the current to a new steady state reflects voltage-dependent changes in the channel open-close equilibrium (*14*). Homomeric GluR-B channels (Fig. 4A) showed small current relaxations and gave instantaneous *I-V* relations that were slightly less curved than steady-state *I-V* curves constructed by voltage ramp or holding potential methods. Thus, the channels formed by GluR-B subunits may have linear or only slightly outwardly rectifying *I-V* relations, indicating that their conductance is almost independent of voltage. The currents measured from homomeric GluR-D channels also showed only small current relaxations (Fig. 4B), and the instantaneous *I-V* curves were inwardly rectifying. This indicates that the conductance of GluR-D channels is voltage-dependent and probably underlies the shape of the steady-state *I-V* relations. GluR-A channels also displayed inwardly rectifying instantaneous *I-V* curves. GluR-B/D channels exhibited larger current relaxations but nearly linear instantaneous *I-V* relations (Fig. 4C). These data suggest that differences in the steady-state *I-V* relations of homomeric GluR-B channels and homomeric GluR-A and -D (and presumably GluR-C) are predominantly due to differences in the voltage dependence of the channel conductances. The dominance of the GluR-B subunit in heteromeric channels may be due to its dominance in determining the voltage dependence of channel conductance. However, because the single-channel *I-V* relations were not directly measured, the possibility exists that these differences are due to very rapid (< 1 ms) voltage-dependent channel gating.

Our results indicate that the ion transport properties of recombinant GluR channels are critically determined by the amino acid sequence of the putative transmembrane segment TM2 as previously assigned (*2, 5, 6*). An arginine residue within this segment located close to the extracellular end produces channels with outwardly rectifying *I-V* relations in homo- and heteromeric assemblies of GluR-polypeptides. Rectification of channel conductance in nicotinic acetylcholine receptors (AChRs) is dependent on various amino acid residues in the M2 transmembrane segment of AChR subunits (*15*). When the net charge of a ring of amino acids on the extracellular side of M2 is made more positive, the negative limbs of the *I-V* curves become less steep. The results we have obtained could be interpreted similarly. Making the charge of the TM2 segment more positive by exchanging these particular residues (glutamine to arginine) results in less steep *I-V* relations at negative voltages. Thus, the results support the view that the TM2 segment of GluR polypeptides crosses the membrane and forms part of the ion channel.

Most native AMPA receptors have linear or outwardly rectifying *I-V* relations (*16*). Our results suggest that such receptors contain at least a GluR-B subunit. However, other subunits that act like GluR-B may yet be found. Conversely, a subpopulation of cultured hippocampal neurons exhibit kain-

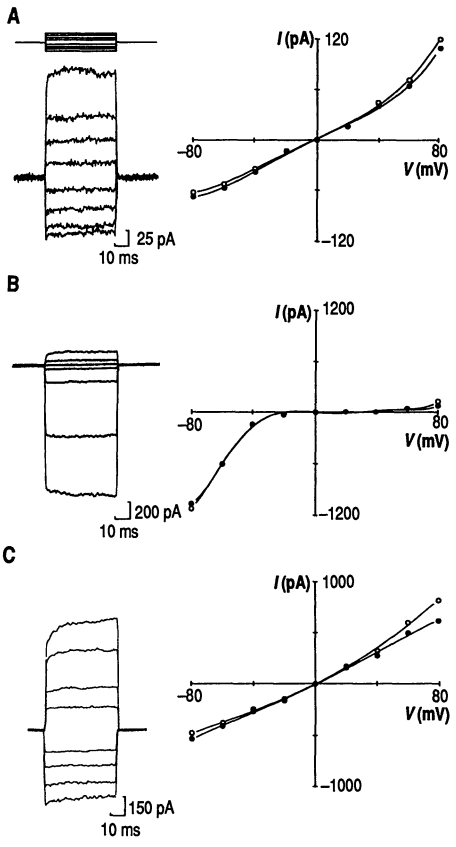

Fig. 4. Voltage-dependent channel conductances determine the difference in steady-state *I-V* relations between GluR-B and GluR-D channels. *I-V* curves were constructed by the voltage jump method (*13*) in cells expressing GluR-B (**A**), GluR-D (**B**) or GluR-B/D (**C**) channels. The current traces in response to voltage jumps (shown schematically above the current traces) from 0 mV to ±80, ±60, +40, and ±20 mV are shown on the left. The resulting instantaneous (●) and late (○) *I-V* curves are shown on the right. The solid lines represent the fit of the data to polynomial equations. For GluR-B and GluR-B/D channels, the late *I-V* curves rectified more than the instantaneous *I-V* curves. The rectification ratio (G_{+80}/G_{-80}) for GluR-B in this case was 1.85 for the late current and 1.55 for the instantaneous current. The cell expressing GluR-B/D channels gave ratios of 1.72 (late) and 1.2 (instantaneous). The ratio for GluR-D was 0.08 and essentially the same for the peak and instantaneous current. Similar results were obtained in two to three other cells for each subunit combination.

Table 2. *I-V* relation of mutant GluRs. Summary of results obtained from steady-state *I-V* curves determined for GluRs composed of at least one mutant GluR subunit. See legend to Table 1 for description.

Subunit combination	V_{rev} (mV)	G_{+80}/G_{-80}	
		L-Glutamate (300 μM)	Kainate (300 μM)
GluR-B(R586Q)	−3.4 ± 5.2 (6)	0.106 ± 0.042 (6)	0.055 ± 0.031 (4)
GluR-D(R587Q)	3.8 ± 3.4 (3)	1.52 ± 0.10 (3)	1.63 ± 0.13 (5)
GluR-B/D(Q587R)	−6.8 ± 12 (3)	1.65 ± 0.28 (3)	1.56 ± 0.18 (3)
GluR-B(R586Q)/D	−19, 2.3 (2)	0.058, 0.830 (2)	0.023, 0.31 (2)
GluR-B(R586Q)/D(Q587R)	2.3 ± 0.9 (5)	1.44 ± 0.15 (5)	1.61 ± 0.20 (5)
GluR-A/B(R586Q)	−11 ± 5.4 (3)	0.27 ± 0.10 (3)	0.12 ± 0.06 (4)
GluR-A/D(Q587R)	4.2 ± 1.5 (3)	1.08 ± 0.08 (3)	1.59 ± 0.15 (3)
GluR-B/B(R586Q)	−3.8 ± 7.4 (3)	2.32 ± 0.28 (3)	2.35 ± 0.14 (3)
GluR-D/D(Q587R)	−0.41 ± 1.2 (4)	1.14 ± 0.08 (4)	1.86 ± 0.05 (4)

ate-induced currents with marked inward rectification (*17*). These GluRs probably lack a GluR-B subunit. The properties of heteromeric GluRs (having at least GluR-B) are comparable to those of native non-NMDA GluRs, for example, in hippocampal neurons. The *I-V* curve for the peak current is less curved than that for the steady-state current in GluRs native to rat hippocampal CA3 pyramidal neurons, and the desensitization rate of these hippocampal GluRs is similar to that of heteromeric GluR-A/B (*18*). Excitatory postsynaptic currents in pyramidal neurons of the CA1 (*19*) and CA3 (*20*) region also show linear *I-V* relations. It seems likely that the voltage-dependent properties of excitatory postsynaptic currents mediated by non-NMDA GluRs are determined by the GluR-B subunit.

REFERENCES AND NOTES

1. D. T. Monghan, R. J. Bridges, C. W. Cotman, *Annu. Rev. Pharmacol. Toxicol.* **21**, 165 (1989).
2. K. Keinänen *et al.*, *Science* **249**, 556 (1990).
3. M. Hollman *et al.*, *Nature* **342**, 643 (1989); T. L. Dawson, R. A. Nicholas, R. Dingledine, *Mol. Pharmacol.* **38**, 779 (1990).
4. J. Boulter *et al.*, *Science* **249**, 1033 (1990).
5. N. Nakanishi, N. A. Shneider, R. Axel, *Neuron* **5**, 569 (1990).
6. K. Sakimura *et al.*, *FEBS Lett.* **272**, 73 (1990).
7. B. Sommer *et al.*, *Science* **249**, 1580 (1990).
8. Human embryonic kidney cells were cultured and transfected essentially as described [T. A. Verdoorn, A. Draguhn, S. Ymer, B. Sakmann, P. H. Seeburg, *Neuron* **4**, 919 (1990)]. Patch-clamp recordings were made in the whole-cell configuration [O. P. Hamill, A. Marty, E. Neher, B. Sakmann, F. Sigworth, *Pfluegers Arch.* **391**, 85 (1981)]. During experiments, cells were continuously perfused with extracellular solution consisting of 135 mM NaCl, 5.4 mM KCl, 1.0 mM $MgCl_2$, 1.8 mM $CaCl_2$, and 5 mM Hepes, pH 7.2, and the pipette solution was composed of 140 mM CsCl, 1.0 mM $MgCl_2$, 11 mM EGTA, and 10 mM Hepes, pH 7.3. Glutamate and kainate were dissolved in extracellular solution and applied to the cell with a piezo-driven double-barreled system for rapid application (7).
9. The shape of agonist-induced *I-V* relations was quantified by fitting of the data points to a polynomial equation. Fourth order polynomials were sufficient to fit the simple outwardly rectifying *I-V* curves, but tenth-order equations were often necessary for description of the more complex doubly rectifying curves. These polynomials were used for calculation of the reversal potential and chord conductances at particular membrane potentials.
10. Ramp *I-V* curves were constructed by application of a ramp voltage command that went from 0 to ±120 mV in 2 s. Data obtained in the absence of agonist were subtracted from those acquired during the steady-state component of the agonist response to produce agonist-activated *I-V* curves. Digitized data points were averaged over 4 mV, and the average values were used for fitting to polynomials.
11. C. Tang, M. Dichter, M. Morad, *Science* **243**, 1474 (1989).
12. Site-directed mutagenesis of cloned GluR-B and GluR-D flip cDNAs (7) was performed by standard methods [P. H. Seeburg *et al.*, *Nature* **312**, 71 (1984)], with the use of single-stranded DNA as a template [J. Vieira and J. Messing, *Methods Enzymol.* **153**, 3 (1987)]. The following oligonucleotides were used for introduction of changes into coding sequences: 5′-TATCGCATCCCTGTTGCATGAAGGCACCC-3′ (GluR-B 586R to 586Q) and 5′-TGTCACATCCTTGCCTCATAAAGGC-3′ (GluR-D 587Q to 587R). Both oligonucleotides were used to prime the synthesis of the noncoding DNA strand and introduced the three underlined nucleotide changes into the wild-type sequence. Mutants were sequenced across the altered region.
13. Voltage jump experiments were used to estimate the voltage dependence of the single-channel conductance in whole-cell recording because the single-channel conductance of these GluRs is low (<3 pS), presenting difficulties in direct measurement of channel amplitudes. From a holding potential of 0 mV the voltage was stepped to various test voltages for 50 ms. Currents occurring in response to voltage steps applied in the absence of agonist were digitally subtracted from those recorded during the steady-state component of the agonist response. Four to six such subtracted current records were averaged for display and measurement. Currents during the voltage pulse were fit to the equation $I = I_o e^{-t/\tau} + B$, where t = time, τ = apparent time constant of decay, and I_o = extrapolated current amplitude at the start of the voltage pulse (instantaneous current). B was set to the current amplitude reached at the end of the pulse. I_o was taken to represent the instantaneous current, and B was used for the late current amplitude in the *I-V* curves in Fig. 4. If the current during a step showed no obvious relaxation, it was fit to a straight line. The line was extrapolated to the beginning and end of the pulse, and these values were used for the instantaneous and late currents, respectively. Currents were filtered at 4 kHz (−3 dB) before being digitized at 10 kHz. Leak and capacitive currents prevented accurate measurement of agonist currents within 1 ms of a step voltage change.
14. P. R. Adams, *Br. J. Pharmacol.* **53**, 308 (1975); E. Neher and B. Sakmann, *Proc. Natl. Acad. Sci. U.S.A.* **72**, 2140 (1975); R. E. Sheridan and H. A. Lester, *ibid.*, p. 3496.
15. K. Imoto *et al.*, *Nature* **335**, 6191 (1988); A. Villarroel, S. Herlitze, M. Koenen, B. Sakmann, *Proc. R. Soc. London Ser. B* **243**, 69 (1991).
16. M. L. Mayer and G. L. Westbrook, *Prog. Neurobiol.* **28**, 197 (1987).
17. M. Iino, S. Ozakawa, K. Tsuzuki, *J. Physiol. (London)* **424**, 151 (1990).
18. P. Jonas and B. Sakmann, *ibid.* (abstr.), in press.
19. P. Sah, S. Hestrin, R. A. Nicoll, *ibid.* **430**, 605 (1990).
20. P. Jonas and B. Sakmann, in preparation.

21. We thank U. Warncke and M. Kaiser for technical assistance, B. Werner for typing the manuscript, B. Sommer for help with plasmid construction, and D. Colquhoun, P. Jonas, and J. P. Ruppersberg for helpful discussion. Supported by the Alexander von Humboldt Foundation (T.A.V.).

8 March 1991; accepted 30 April 1991

Facilitation of the Induction of Long-Term Potentiation by $GABA_B$ Receptors

DAVID D. MOTT* AND DARRELL V. LEWIS

Long-term potentiation (LTP), an in vitro model of learning, was induced in hippocampal slices by 5-hertz stimulation. During induction, γ-aminobutyric acid A ($GABA_A$) inhibition decreased, causing the *N*-methyl-D-aspartate receptor–mediated excitation to increase. 2-OH Saclofen, a $GABA_B$ receptor antagonist, prevented the reduction of inhibition, the increase of excitation, and the induction of LTP. Therefore, disinhibition caused by $GABA_B$ receptors is required for induction of LTP by 5-hertz stimulation. $GABA_B$ receptor modulation of synaptic plasticity occurs at frequencies in the range of the endogenous hippocampal theta rhythm, which has been shown to modulate LTP in vivo.

LTP, A MODEL OF LEARNING IN THE central nervous system, often requires *N*-methyl-D-aspartate (NMDA) receptor activation (*1*). However, blockade of NMDA channels by Mg^{2+} is normally relieved only by depolarization (*2*). Therefore, LTP is usually induced with stimulus trains of sufficiently high frequency to depolarize the postsynaptic cell.

Inhibition limits postsynaptic depolarization during a stimulus train. When inhibition is blocked with picrotoxin, a $GABA_A$ receptor antagonist, depolarization during a train is enhanced, facilitating LTP induction (*3*). Although blockade of inhibition facilitates LTP, it is unclear if disinhibition is normally required for LTP induction. Inhibition can be reduced by "priming" stimulation (*4*). Priming is so effective that LTP can be produced with as few as two to three stimuli delivered about 200 ms after a single priming stimulus (*4, 5*). In addition, the interstimulus interval for the production of LTP with priming stimulation approximates the periodicity of the hippocampal theta rhythm, which has been linked with LTP in vivo (*5, 6*). We report that $GABA_B$ receptor–mediated disinhibition is required for LTP induction with stimulation in the frequency range of the theta rhythm.

We performed experiments using standard procedures (*7, 8*) in the dentate gyrus of rat hippocampal slices maintained in a submersion chamber perfused with artificial cerebrospinal fluid (ACSF). Responses of granule cells to electrical stimulation of the medial perforant path in the inner two-thirds of the molecular layer were recorded intracellularly.

D. D. Mott, Department of Pharmacology, Duke University Medical Center, Durham, NC 27710.
D. V. Lewis, Departments of Pediatrics (Neurology) and Neurobiology, Duke University Medical Center, Durham, NC 27710.

*To whom correspondence should be addressed.